Shape optimization of the X0-specimen for biaxial experiments

Jan Liedmann[1,*], **Steffen Gerke**[2], **Franz-Joseph Barthold**[1], and **Michael Brünig**[2]

[1] Lehrstuhl Baumechanik, Technische Universität Dortmund, August-Schmidt-Str. 8, 44227 Dortmund, Germany
[2] Institut für Mechanik und Statik, Universität der Bundeswehr München, Werner-Heisenberg-Weg 39, 85579 Neubiberg

The mechanical damage and fracture behavior of ductile sheet metals strongly depend on the stress state and intensity. Thus, for adequate characterization of the material behavior, it is crucial to have specimens that cover different and preferably distinct stress states, especially in the inelastic domain. In this paper, the geometry of the X0-specimen is optimized to achieve a distinct stress triaxiality distribution in the region of damage and fracture occurrence, depending on two different load cases in a biaxial testing environment. The shape optimization is gradient based and the gradients of the objective and constraint functions are computed analytically by means of variational principles. The resulting geometries show improvements in terms of the intensity of the stress state numerically as well as experimentally.

1 Introduction

Ductile sheet metals play an important role in several engineering disciplines. The demand of improvements in terms of weight, cost and energy consumption is growing. Appropriate characterization of the material behavior - especially during inelastic deformations - is essential. This knowledge helps to prevent localization of irreversible strains in an early state of deformation, which leads to material degradation. These effects strongly depend on the stress state and intensity. A high tensile dominated state triggers nucleation and growth of micro-voids, whereas micro-cracks occur in a shear dominated stress state. The stress triaxiality η and Lode parameter ω, defined by

$$\eta = \frac{\sigma^{\mathsf{m}}}{\sigma^{\mathsf{eq}}} = \frac{I_1}{3\sqrt{3\,J_2}} \quad \text{and} \quad \omega = \frac{2\,\tau_2 - \tau_1 - \tau_3}{\tau_1 - \tau_3}, \quad \text{with} \quad \tau_1 \geq \tau_2 \geq \tau_3, \tag{1}$$

characterize the stress state. Here, I_1 and J_2 denote the first and second deviatoric invariant of the Kirchhoff stress tensor and τ_i are the principle Kirchhoff stress components. New biaxial test specimens have been developed in [2] that cover a wide range of stress triaxialities depending on the load case. Shape optimization of the presented specimens promises even more homogeneous and distinct stress states and can be conducted efficiently within a finite element framework based on gradients gained by a variational approach, see e.g. [1, 4].

2 Optimization tasks

The goal of the shape optimization is to improve the stress triaxiality intensity and homogeneity in the notched specimen area. Two different load cases are considered, i.e. ($\bar{u}_1=1$ / $\bar{u}_2 = 1$) producing high stress triaxialities and ($\bar{u}_1=-1$ / $\bar{u}_2 = 1$) producing low stress triaxialities. With the geometric design vector $\mathbf{s}$, the optimization task for both load cases can be written as

$$\min_{\mathbf{s} \in \mathbb{R}^n} J(\mathbf{u}(\mathbf{s}), \mathbf{s}), \quad \text{subject to} \quad \mathbf{c}^{\mathsf{in}} \leq \mathbf{0}, \quad \mathbf{c}^{\mathsf{eq}} = \mathbf{0}, \tag{2}$$

where J denotes the objective function and $\mathbf{c}^{\mathsf{eq}}$ and $\mathbf{c}^{\mathsf{in}}$ denote the vectors of equality and inequality constraints, respectively. Depending on the load case, the objective function is chosen as

$$J(\mathbf{u}(\mathbf{s}), \mathbf{s}) = \pm\|\boldsymbol{\eta}^{\mathsf{cs}}\|, \quad \text{with a negative sign for (1/1) and a positive sign for (-1/1)}, \tag{3}$$

where the vector $\boldsymbol{\eta}^{\mathsf{cs}}$ collects the values of stress triaxiality in the cross section of the notched specimen area, obtained by the solution of the mechanical analysis problem. One equality constraint is chosen to keep the cross section area constant and three inequality constraints prevent destruction of the finite element mesh, viz.

$$c^{\mathsf{eq}} = A^{\mathsf{cs}} - 12\,\mathrm{mm}^2 = 0, \quad \mathbf{c}^{\mathsf{in}} = \begin{bmatrix} R_t - R_i \\ R_t - R_o \\ D - R_t \end{bmatrix} \leq \mathbf{0}. \tag{4}$$

The mechanical analysis problem is given by the elastoplastic initial boundary value problem based on a multiplicative kinematic assuming a plastic stress free configuration given by $\mathbf{F}_{\mathsf{p}} = \mathbf{F}_{\mathsf{e}}^{-1}\,\mathbf{F}$, see [5], and is solved using the finite element method.

---

* Corresponding author: e-mail jan.liedmann@tu-dortmund.de, phone +49 231 755 7244, fax +49 231 755 7244, ORCID iD 0000-0001-8759-6940
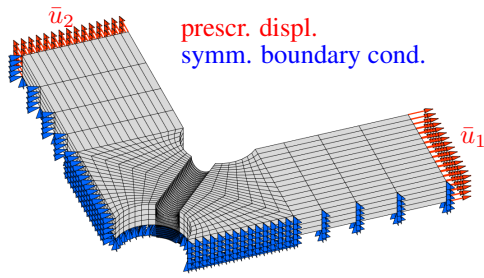
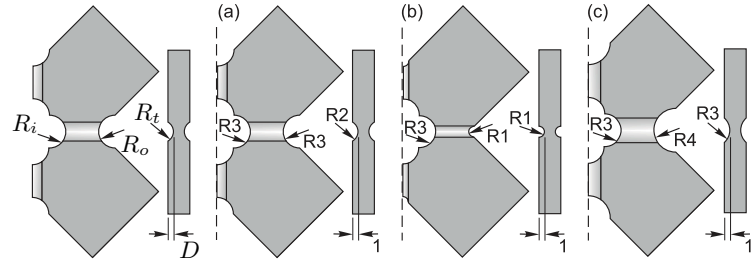**Fig. 1:** Initial finite element mesh

Fig. 2: Design values. (a) Initial geometry, (b) Optimized for load case (1/1), (c) Optimized for load case (-1/1)

For the gradient based solution of the inverse problem given in Sec. 2, the gradient of the objective function is computed based on the variational approach explained in e.g. [1, 4]. The total variation of the stress triaxiality reads

$$\delta\eta = \frac{1}{\sigma^{\mathsf{eq}}} \left(\frac{1}{3}\,\mathbf{I} - \frac{3\,\eta}{2\,\sigma^{\mathsf{eq}}}\,\boldsymbol{\tau}_{\mathsf{dev}} \right) : \delta\boldsymbol{\tau}, \quad \text{with} \quad \delta\boldsymbol{\tau} = \frac{\partial\boldsymbol{\tau}}{\partial\mathbf{u}}\,\delta\mathbf{u} + \frac{\partial\boldsymbol{\tau}}{\partial\mathbf{s}}\,\delta\mathbf{s} + \frac{\partial\boldsymbol{\tau}}{\partial\mathbf{h}_n}\,\delta\mathbf{h}_n, \tag{5}$$

where the total variation of the Kirchhoff stress tensor $\delta\boldsymbol{\tau}$ is obtained considering the fact that the weak equilibrium condition ($R = 0$) has to hold for any geometric design change. The discrete version of the total variation of the weak equilibrium reads

$$\delta\mathbf{R} = \mathbf{K}\,\delta\mathbf{u} + \mathbf{P}\,\delta\mathbf{s} + \mathbf{H}\,\delta\mathbf{h}_n \stackrel{!}{=} \mathbf{0} \quad \text{and therefore,} \quad \delta\mathbf{u} = -\mathbf{K}^{-1}\,(\mathbf{P}\,\delta\mathbf{s} + \mathbf{H}\,\delta\mathbf{h}_n) = \mathbf{S}\,\delta\mathbf{s}, \tag{6}$$

which yields the sensitivity matrix $\mathbf{S}$ connecting the structural response with geometric design changes, cf. [4]. The values of variations of history variables $\delta\mathbf{h}$ have to be saved and updated in each load increment within the finite element procedure.

3   Numerical investigations

The finite element mesh consisting of 5376 $\bar{F}$-elements is shown in Fig. 1. The design variables stored in the design vector $\mathbf{s}$ are three radii and the penetration depth of the notch in thickness direction. In Fig. 2 the values of the four geometric design variables are summarized for the initial and the optimized geometries depending on the specific load case. The stress triaxiality distributions for the (1/1) and (-1/1) load case are illustrated in Fig. 3 and Fig. 4, respectively. For the (1/1) load case, an improvement can be clearly observed, while for the (-1/1) load case, the stress triaxality distribution is very similar.
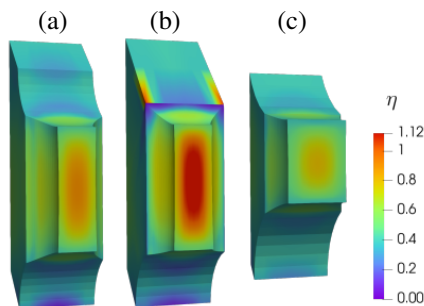

Fig. 3: Stress triaxiality distribution for load case (1/1)
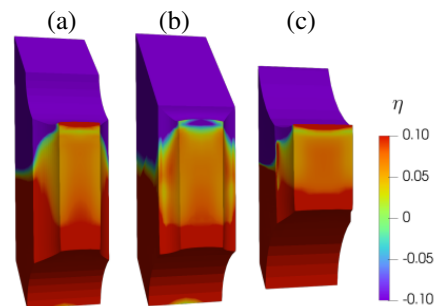

Fig. 4: Stress triaxiality distribution for load case (-1/1)

4   Concluding remarks

For verification of the results obtained by the presented shape optimization procedure, the resulting optimized X0 geometries have been fabricated and compared to the initial X0 geometry. The biaxial test series has been captured by digital image correlation (DIC) and the fracture surfaces have been examined by scanning electron microscopy (SEM). It can be seen that the fracture surface of the optimized geometry for the (1/1) load case exhibits significantly larger voids due to the higher stress triaxiality. More details on the experimental investigations can be found in [3].

PAMM · Proc. Appl. Math. Mech. **20**:1 (2020)

3 of 3

References

[1] F.-J. Barthold, Braunschweiger Schriften zur Mechanik **44**, (2002).

[2] S. Gerke, P. Adulyasak and M. Brünig, International Journal of Solids and Structures **110**, 209-218 (2017).

[3] S. Gerke et al., Damage and fracture of the optimized X0-specimen, PAMM **20**, (2020).

[4] J. Liedmann and F.-J. Barthold, Structural and Multidisciplinary Optimization **61(6)**, 2237-2251 (2020).

[5] J. Simo, T. J. R. Hughes, Computational Inelasticity, (2000).